Journal of Structural Geology, Vol. 15, No. 1, pp. 37 to 53, 1993
Printed in Great Britain

0191-8141/93 $06.00 + 0.00

Neogene evolution of the Denizli region of western Turkey

ROB WESTAWAY

Department of Geological Sciences, University of Durham, Durham DH1 3LE, U.K.

(*Received* 16 *January* 1992; *accepted in revised form* 15 *June* 1992)

Abstract—The Denizli region contains one of the easternmost Neogene sedimentary basins in the part of western Turkey that takes up SSW extension. This isolated active normal fault zone, which contains closely spaced en échelon normal fault branches, is investigated using field measurements of fault exposures and tilted sediments, and seismological observations, as a case study to address its style of extension. The Denizli basin is no more than ~1 km thick and has accommodated up to 4 km of extension. Substantial (~20°) sediment dips are readily explicable assuming extension is accompanied by distributed vertical simple shear, with initial and present-day dips of the main normal faults that control extension most likely 54–57° and 45–50°. Other aspects of the form of this basin require regional uplift at ~0.1 mm yr^{-1}, providing the first indication of major tectonic elevation changes in this actively-extending region that are not directly related to throw on normal faults.

INTRODUCTION

THE Denizli Neogene sedimentary basin is situated within the extensional province that covers western Turkey, the Aegean Sea, and most of Greece. It is near the eastern end of the Büyük Menderes, Küçük Menderes and Alaşehir fault zones that take up much of the extension of westernmost Turkey (e.g. Westaway 1990a) (Fig. 1). The Denizli basin is 50 km long and up to 24 km wide, bounded by major NNE-dipping normal faults at its southwestern margin (e.g. Koçyiğit 1984, Westaway 1990a), which have taken up NNE extension, and by other normal faults that dip SSW. Its central depocentre is flanked by uplifted Neogene sediment that is well exposed as a result of the arid climate. Recent moderate-sized normal-faulting earthquakes (e.g. McKenzie 1972, Westaway & Smith 1989a; see Appendix 1) and destructive historical events (e.g. Baumgarten 1987, pp. 197 and 204) confirm that this basin is actively extending.

The outcrops around Denizli have been studied by many people since the first detailed report by de Tchihatscheff (1867), who recognized the uplifted Neogene basin and described its fossiliferous brackish-water marl sediments (Fig. 2). Structural and geophysical studies constrain the nature of the basin interior at depth (e.g. Tezcan 1979). The regional guide by Pamır & Erentöz (1974) and its copious bibliography provide the basis for the present paper, which examines relationships between tilting of beds and dips of active normal faults within this basin, and estimates the extension across it. This article describes field observations that quantify this extension and its partitioning between individual normal faults. They comprise striations on normal fault planes that constrain extension direction, dips of beds that give the tilting during extension, and present-day elevations of marine sediments that indicate tectonic elevation changes since deposition.

Several reasons make the Denizli basin useful for testing general models of extension. (1) Much of it is accessible by the roads serving Denizli city (population ~200,000). (2) The crystalline limestone basement in normal fault footwalls near its eastern end forms cemented breccia on fault planes, in which striations reveal slip sense. In contrast, in many other localities in western Turkey normal faults offset schist that weathers rapidly and does not preserve fault surfaces well. (3) The exposed marl almost certainly had negligible depositional dip, so present-day dip is most likely caused by subsequent tilting. This contrasts with the typical clastic sedimentation in most other Neogene basins in western Turkey, much of which is in alluvial fans, where some depositional dip is possible. (4) Cross-sections perpendicular to strike do not intersect other major active normal faults for tens of kilometres in the surroundings of the Denizli basin. No other major normal faults thus need be considered when describing its present-day form. (5) Local extension is shown to be subperpendicular to the strikes of the principal normal faults, and potential complications associated with restoring oblique extension thus do not affect this basin. (6) No significant tectonic activity appears to have occurred locally for $\geq$10 Ma before the start of the present phase of extension (e.g. Pamır & Erentöz 1974), which appears to have begun in middle–upper Miocene time. It is thus relatively easy to distinguish features that date from this deformation phase. This contrasts with other parts of western Turkey and adjacent offshore areas of Greece, where different senses of deformation appear to have been occurring immediately before the present phase started (e.g. Poisson 1977, Gutniç *et al.* 1979, Kaya 1981, Mercier *et al.* 1989). (7) The Denizli basin was connected to the sea during the early stages of extension. Present-day elevations of these marine sediments indicate subsequent absolute elevation changes. (8) Although other Neogene basins in western Turkey have recently been studied in detail (e.g. Roberts 1988, Price & Scott 1991, Seyitoğlu & Scott 1992, Taymaz & Price 1992), Denizli has received little attention.

This study was motivated both to investigate this

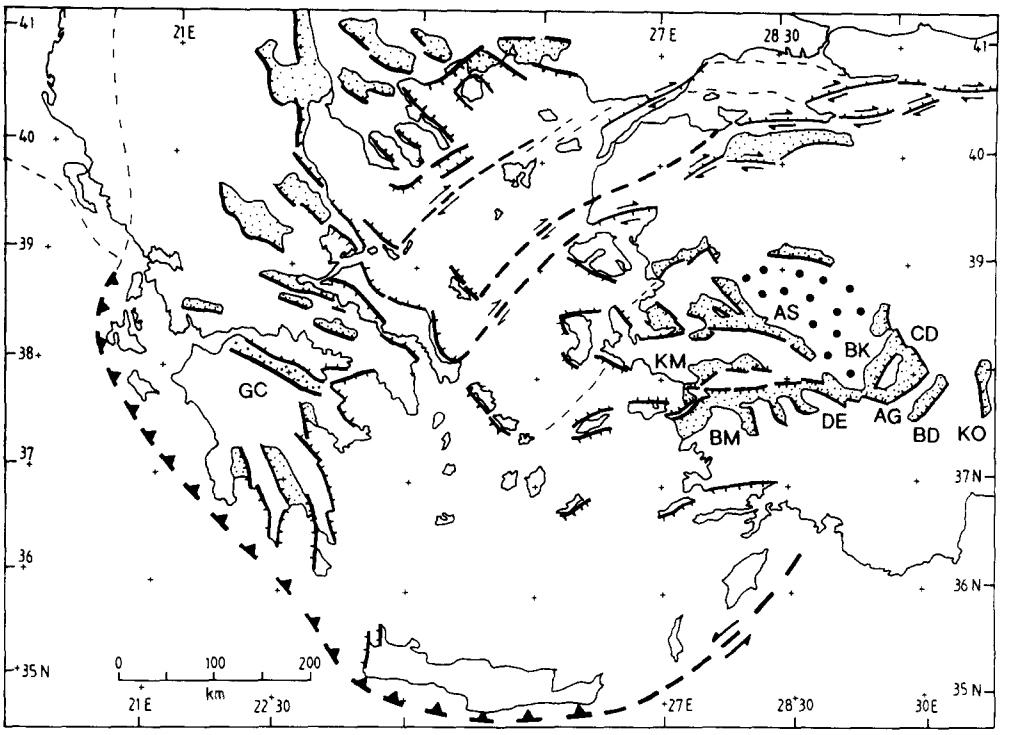

Fig. 1. Summary map of the Aegean Sea region showing some of the principal actively evolving sedimentary basins (stippled where on land), active normal faults (with hanging-wall ticks), strike-slip faults within the North Anatolian fault zone (with paired arrows), and the schematic surface trace of the Hellenic Benioff zone (with chevrons in the overlying plate). Dashed lines within strike-slip fault zones outline pull-apart basins. Dashed lines west of the Turkish coast indicate a possible additional branch of the North Anatolian fault zone suggested by Taymaz *et al.* (1991). The dashed lines at the northern continuation of the Hellenic Benioff zone indicate schematically the zone of shortening between the Eurasian and African plates. The Denizli basin (DE) is shown in relation to its surroundings. BM, KM and AS denote the Büyük Menderes, Küçük Menderes and Alaşehir fault zones; GC denotes the Gulf of Corinth; AG, BD, BK, CD, and KO denote the Açıgöl, Burdur, Baklan, Çatma Dağı and Kovada faults. The Gelendost fault is ~30 km east of the Kovada fault. Solid circles denote land at uniform ~900 m elevation north of the Denizli basin. Based on information from Le Pichon *et al.* (1984), Barka & Kadinsky-Cade (1988), Turgut (1988), Westaway (1990a), Roberts & Jackson (1991) and Taymaz *et al.* (1991).

particular basin and to test general models for extension of the brittle upper crust. I noticed the substantial dips of its Neogene sediments during my first visit in 1988. However, I initially precluded a tectonic cause, believing that the evidently limited local extension should require less tilting. Subsequent developments in theoretical modelling (e.g. Westaway & Kusnir 1990, in press) can predict greater bed tilting in localities with limited extension. This theory can now be applied to the Denizli basin (and other localities), to show that these dips are related to tectonics.

The critical issue addressed by Westaway & Kusznir (in press) is whether tilting of the surroundings of closely-spaced normal faults is better described as *distributed vertical simple shear* or as *rigid-body rotation*. If one denotes initial and final dips of a fault by δ_0 and δ (with $\psi = \delta_0 - \delta$) and dip of the oldest hanging-wall sediments near this fault (or the dip of any other surface, such as an erosion surface or unconformity, which was horizontal when extension began) by θ, then for rigid-body rotation:

$$\theta = \delta_0 - \delta = \psi. \tag{1}$$

For example, if the steepest beds in a basin dip at 15°, and the normal fault at its margin dips at 45°, this assumption predicts initial fault dip 60°. An angle κ can be defined as $\theta - \psi$, the difference between angles of tilting of a normal fault and adjacent beds. For rigid-body rotation κ is thus always zero.

The assumption of distributed vertical simple shear predicts instead that:

$$\tan\theta = \tan\delta_0 - \tan\delta \tag{2}$$

(see Westaway & Kusznir in press). Following this assumption, if beds dip at 15° near a normal fault with dip 45°, the fault had initial dip 52°, not 60° as before. Equation (2) can be rewritten in terms of ψ and then rearranged to give:

$$\tan\theta = \frac{\tan\psi\,[1 + \tan^2\delta_0]}{1 + \tan\delta_0 \tan\psi}. \tag{3}$$

Equation (3) can then be rewritten as $\tan\theta = f\tan\psi$, where

$$f = \frac{1 + \tan^2\delta_0}{1 + \tan\delta_0 \tan\psi}. \tag{4}$$

Usually, ψ will be less than δ_0, and hence $f > 1$. This means that κ is greater than 0°, indicating that under vertical shear, bed tilting will usually exceed fault tilting.

Moving away from any isolated normal fault, the dip of any bed will decrease, eventually becoming zero with no other fault present. Equations (2)–(4) relate to dips of beds when adjacent to faults, and thus require dip

measurements in such localities. The distance over which bed tilt decreases, and related parameters such as the radius of curvature of its tilting, depend on the effective elastic thickness of the upper crust (e.g. Kusznir *et al.* 1991, Westaway 1992b), and are not quantifiable simply in terms of geometry.

It is important to note that the assumption of rigid-body rotation does not relate to the physics of deformation of the Earth's crust. However, it has become a familiar model in recent years (e.g. Jackson & McKenzie 1983, Jackson 1987, Jackson & White 1989, Taymaz & Price 1992), despite not having been tested. Recent numerical methods for modelling deformation in the surroundings of normal faults suggest (to a good approximation at least) vertical shear rather than rigid-body rotation (e.g. Kusznir *et al.* 1991). It is thus important to investigate directly whether vertical shear does occur, using case studies with clear angular relationships between fault and bed tilting, but without assuming any particular numerical method (see Westaway & Kusznir in press). The features of the Denizli basin that make it most useful for such a test are shown to be the substantial (~20°) tilting of thin sedimentary sequences and the reversal of tilt polarity over a few kilometres distance (Fig. 4). These observations will be shown to be explicable if extension is accompanied by vertical shear, but not if it is accompanied by rigid-body rotation.

In more central parts of the Aegean region where more extension has occurred, including westernmost Turkey and central Greece, greater tilting is observed in thicker sedimentary sequences (e.g. Westaway 1990a, Roberts & Jackson 1991). For example, uplifted Neogene sediments within the Büyük Menderes fault zone west of Denizli (Fig. 1) dip at up to ~26–30°, and adjacent normal faults that cut the basement dip at ~45° (e.g. Jones & Westaway 1991, Seyitoğlu & Scott 1992). Although these localities are not inconsistent with verti-

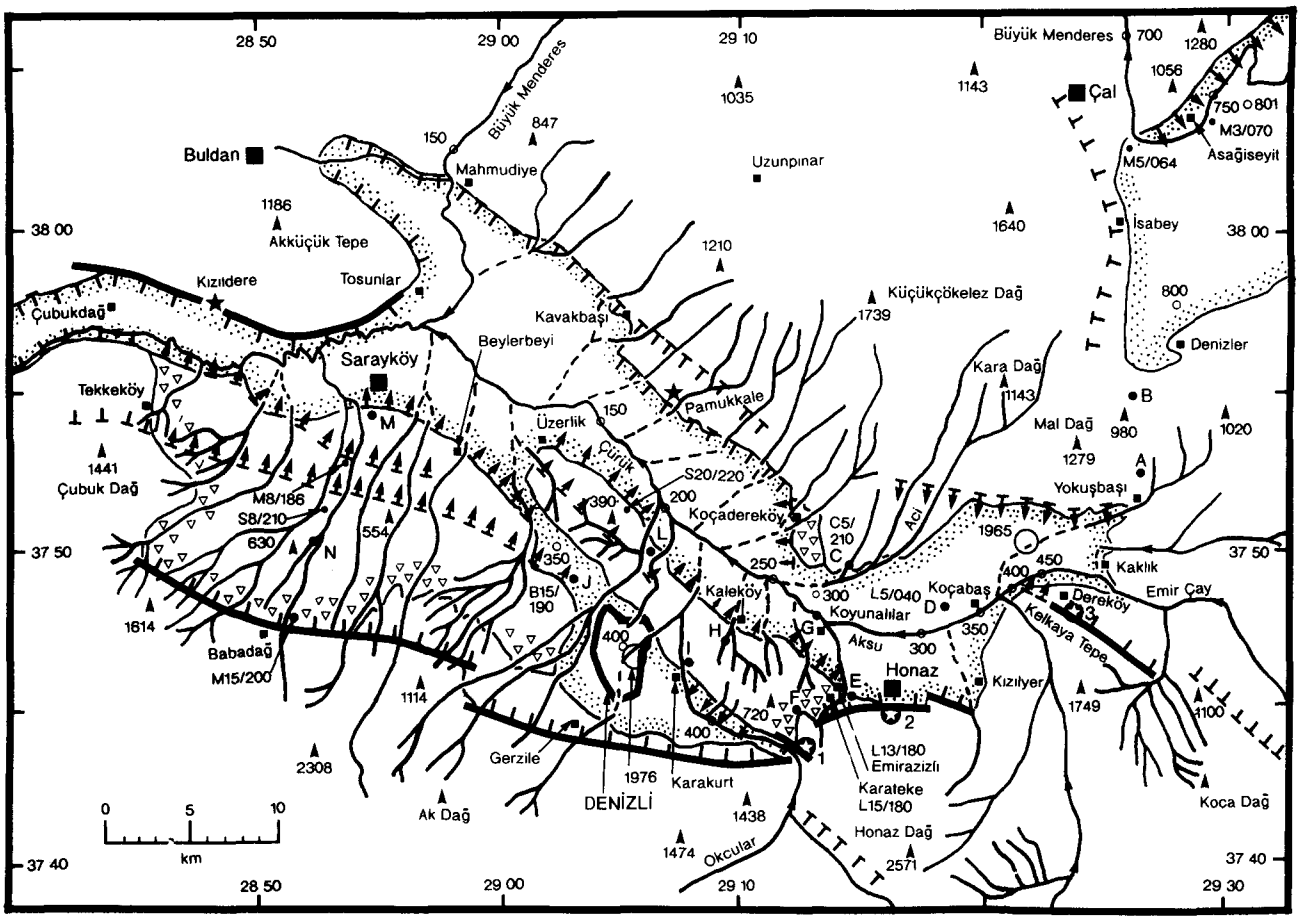

Fig. 2. Map of the Denizli basin, showing simplified outcrop information, topography, active normal faults, drainage, field localities and dip measurements in Neogene sediments. Flat areas in the interiors of the Denizli and Baklan basins, which correspond approximately to depocentres, are outlined with fine dots. Sediments identified by Pamır (1964) as the uppermost Miocene brackish-water facies are outlined by open triangle symbols. Other outcrop is undifferentiated. Star symbols denote the principal hot springs, associated with the Kızıldere geothermal field and the famous Pamukkale travertine. Normal faults are shown with hanging-wall ticks. Localities where unconsolidated sediments appear to overlie or drape over buried faults are shown using similar symbols with arrowheads pointing towards the inferred downthrow. Open circles denote spot heights along rivers or in valley floors; triangles denote summit elevations. 1–3 denote the Okcular, Honaz and Dereköy cemented limestone breccia fault surfaces where striations indicate local slip sense (see text and Table 2), and A-N denote other localities that are mentioned in the text (see also Appendix 2). Dip measurements use the notation Xnn/mmm. Here X denotes the sediment type (C is conglomerate, L is limestone, M is marl and S is sandstone), and nn and mmm are the dip and down-dip azimuth, both in degrees. To avoid clutter, most detail from the Kaleköy and Laodikeia localities (localities H–I and L) is omitted from this figure (see Figs. 4 and 5 instead). The cross-sections in Fig. 6 run from Gerzile in the south (immediately south of Denizli city) to Pamukkale in the north.

cal shear, it is more difficult to establish this uniquely as the cause of their present-day forms. Where extension is minimal, such as near the eastern edge of the extensional province in western Turkey (Westaway 1990a), and in central Italy (e.g. Westaway *et al.* 1989), bed and fault tilting are also minimal. Such localities constrain initial dips of normal faults (Table 2), but do not directly help to distinguish vertical shear and rigid-body rotation. The Burdur basin east of Denizli (Fig. 1) provides another potential case study. Its lower Pliocene lacustrine sediments typically tilt at 13° (Price & Scott 1991, Taymaz & Price 1992), and the adjacent normal faults that cut basement typically dip at ~50–62°. However, this basin appears to have been isolated since local extension began, and thus lacks the control on elevation that is provided by marine sediments at Denizli.

FIELD OBSERVATIONS

Stratigraphy and outcrop observations

Many people have proposed terminology for the Neogene of western Turkey, using lithostratigraphy, biostratigraphy or other methods. Others have tried to correlate the numerous independent nomenclatures from different localities (see e.g. table 1 of Sickenberg & Tobien 1971). In some cases local observations have been interpreted using regional stratigraphic classifications for eastern Europe or the eastern Mediterranean, which have uncertain relationships to global terms. Some such correlations need careful scrutiny following later changes to the accepted time scale. In particular, many early studies regarded the Pannonian stage as lower Pliocene, rather than the early part of the upper Miocene as is now accepted.

Seyitoğlu & Scott (1991) have tried to reconcile some of these local nomenclatures both with absolute dates and with standard geological time scales. This complex issue depends on being able to develop a regional time scale using microfossils in sedimentary sequences within extensional basins, then calibrate it by radiometric dating of volcanic rocks that mostly occur elsewhere. Until recently, evidence from western Turkey and nearby localities led to the view that extension began during Tortonian time (~7–11 Ma), probably near its start (e.g. Kaya 1981, Şengör *et al.* 1985, Sen & Valet 1986, Şengör 1987). The revised chronology proposed by Seyitoğlu & Scott (1991, 1992) suggests instead that this extension began during an interval of a local microfossil time scale that persists between middle Burdigalian and middle Serravallian. Using the time scale of van Eysinga (1978), Burdigalian means ~15–20 Ma and Serravallian ~11–13 Ma, and this estimate for the start of extension thus means ~12–18 Ma. However, Seyitoğlu & Scott (1991, 1992) used a different time scale, from Steininger & Rögl (1984), where middle Serravallian and middle Burdigalian mean ~15 and ~20 Ma. Although the extent is unclear to which different local conditions prevent general stratigraphic correlation between Neogene basins in western Turkey and between these basins and other localities, the sedimentary sequence at Denizli (Fig. 3) has been recognized as unusual, different from others in the region (e.g. Becker-Platen 1971).

Other evidence also bears upon the timing of the start of extension in western Turkey. First, its magmatism becomes mainly alkaline (generally thought to be associated with extension) around ~15 Ma (see compilation of data by Seyitoğlu & Scott 1991). Second, in a review of many parts of the Aegean region, Mercier *et al.* (1989) noted that thrusting was occurring in the southern part of western Turkey until Langhian time (which they took to be ~16 Ma); extension in neighbouring localities thus presumably started later. They regarded the oldest demonstrable extension elsewhere in the Aegean as middle Miocene (Langhian–Serravallian). The start of extension in western Turkey thus appears to be bounded by ~11 and ~20 Ma, with most evidence pointing towards ~15 Ma.

The geology of the Denizli region is summarized in Fig. 2 mainly from Pamır & Erentöz (1974). Basement in much of this region, like further west in Turkey, comprises the Palaeozoic Menderes schist. The southeastern part of the basin is bounded instead by Mesozoic crystalline limestone, which preserves fault surfaces well and thus facilitates interpretation of extension. The complex pre-Neogene evolution of these and other rocks is not

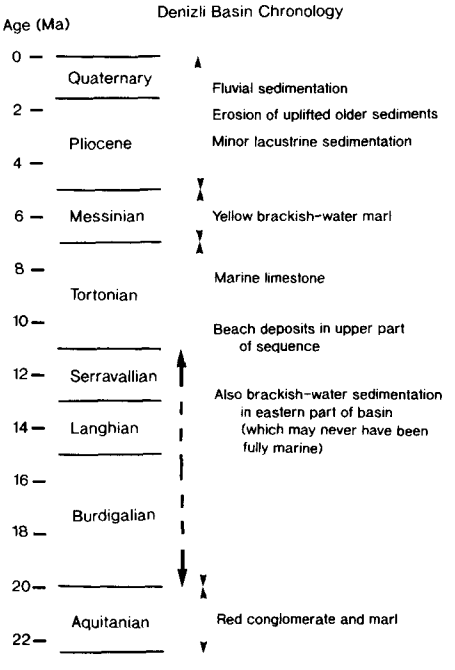

Fig. 3. Summary of my preferred interpretation of the chronology of the Denizli basin. The principal sedimentary processes occurring are shown for different stages of Miocene time, and during Pliocene and Quaternary time. Solid horizontal lines separate these divisions of geological time, using the time scale of van Eysinga (1978). Other studies use different time scales. For example Seyitoğlu & Scott (1991) used alternative dates from Steininger & Rögl (1984): 5.4 Ma (base Pliocene), 7.0 Ma (base Messinian), 11.8 Ma (base Tortonian), 16.0 Ma (base Serravallian), 16.8 Ma (base Langhian), 22.0 Ma (base Burdigalian) and 23.2 Ma (base Aquitanian). Dashed vertical line indicates bounds for the start of extension, about my preferred value of ~15 Ma. Seyitoğlu & Scott (1992) believed the bounds to be tighter, ~14–20 Ma, because of their different age (~14–15 Ma) for the middle Serravallian.

discussed here. During Aquitanian time (lower Miocene; ~22–20 Ma), a distinctive conglomerate, with well-rounded clasts in a red matrix, was deposited over much of the region, and was overlain by red marl. This sequence, which is older than the start of extension, is well exposed near Tavas, ~15 km south of Denizli, and between Kaklık and the Baklan basin (localities A–B in Fig. 2; see also Appendix 2). It is also observed at the base of the Neogene sequence in the Büyük Menderes fault zone (Seyitoğlu & Scott 1992). These red units are unconformably overlain by fossiliferous marine limestone, reportedly of Burdigalian to Helvetian (Tortonian) age (~20 to between 11 and 7 Ma; lower–upper Miocene), which crops out in several prominent localities in the Denizli basin interior (most notably at locality J). Younger whitish-yellow marl crops out in much of the uplifted part of the basin, being found on its southern flank at elevations over 600 m in the west and 700 m in the east, but no higher than 400 m in a small outcrop near Koçadereköy on its northern flank. This has an ostracod fauna typical of a brackish environment. Pamır & Erentöz (1974) regarded it as of Pannonian age, but did not say whether they meant the old usage. Gökçen (1982) concluded that it is probably upper Miocene. A Pliocene sequence rests unconformably on the brackish-water marl in some localities and on older rocks elsewhere. This begins with sandy marl, overlain by lacustrine limestone and later by fluvial conglomerate. Both mollusc fossils and microfauna indicate a transition from brackish to freshwater conditions early in this sequence. The Neogene sequence beneath the depocentre in the western Denizli basin between Sarayköy and Kızıldere (Fig. 2) has been drilled (see Tezcan 1979). Beginning with the red basal units, it is 1100 m thick. The brackish-water marl is well exposed further south along the road from Sarayköy to Babadağ (Fig. 2). Typically, the dip is 8–15°SSW, but intermittently beds tilt NNE at up to 30° for a few hundred metres. These dip changes can be interpreted as points where the marl is draped over blind NNE-dipping normal faults, and thus reveal such faults in this western uplifted part of the basin. Streams incise this marl by up to ~200 m, with basement exposed in one channel at locality N (Fig. 2) ~4 km north of Babadağ.

A 5 km traverse between Kaleköy and Karakurt reveals the form of bed tilting in the eastern part of the basin (Fig. 4 and localities H–I in Fig. 2). Brackish-water marl is exposed for 2 km south of Kaleköy, and forms most of the ~300-m-high escarpment there, with conglomerate with a SSW dip of 20–24° exposed at its top. Further west, sand and marl with SSW dips of 14–24° are exposed along a continuation of this escarpment (Figs. 2 and 5). This local uplift and tilting are explicable as a result of displacement in the footwall of a NNE-dipping normal fault, which I have called the Kaleköy fault, which bounds the active depocentre to the southsouthwest. Immediately south of Kaleköy, limestone with bulrush fossils is well exposed (locality H), and dips SSW at 18°. I am unaware of any study that has dated this outcrop. Its resemblance to the upper Miocene limestone at localities D and G suggests that, like the nearby conglomerates with similar dips, it belongs near the base of the uppermost Miocene sequence. If substantially younger, it has subsided relative to the older sediments above it (see caption to Fig. 4). This other interpretation requires complex local normal faulting for which there is no evidence, and I believe it can be discounted. I thus estimate the steepest typical sediment dips in the footwall of the Kaleköy fault as 20°, reflecting observations in and around localities H and L (Figs. 4 and 5).

Watersheds at ~980 and ~870 m elevation separate the Denizli basin from the adjacent Baklan and Acıgöl basins. The main drainage within the Denizli basin is axial, like in other active normal fault zones in western Turkey: the Aksu and Çürük rivers flow westward, joining the Büyük Menderes River near Sarayköy. The Büyük Menderes drains an upstream area of more than 10,000 km^2. It leaves the Denizli basin at its western end near Çubukdağ, flowing axially along the hanging-wall of the Büyük Menderes fault zone to the Aegean Sea ~150 km further west (Fig. 1). Streams that enter the Denizli basin from the southeast (Fig. 2) drain only ~200 km^2 area, which does not include the nearby Acıgöl basin. Many other streams enter the Denizli basin from both margins typically ~2 km apart, and flow subperpendicular to fault strike across the uplifted sediments, forming a drainage style that also typifies other Aegean normal fault zones (Roberts & Jackson 1991). However, in the eastern part of the southern basin margin only the largest streams flow subperpendicular

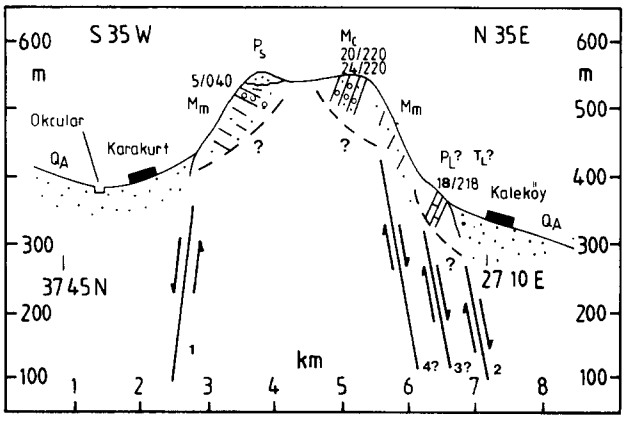

Fig. 4. Cross-section between Kaleköy and Karakurt in the eastern Denizli basin, showing outcrop information and inferred normal faults at 10:1 vertical exaggeration. Outcrop symbols denote the following: Q_A, Quaternary alluvium; P_S, unconsolidated fluvial sandstones (upper (?) Pliocene age); P_L(?) T_L(?) medium hard limestone with bulrush fossils that may either be Pliocene or upper Miocene (probably Tortonian); M_m, yellow-white marl (uppermost Miocene, probably Messinian) (near Karakurt gravel beds in its upper part enable its orientation to be measured); M_c, well-consolidated conglomerate (uppermost Miocene, probably Messinian). Thick lines with arrows suggest active normal faults. The fluvial sands are cross bedded and true dip cannot be measured with confidence. The section has three possible interpretations: First, slumping in landslides may cause tilting. Dashed lines denote positions of possible landslides. Second, the Kaleköy escarpment is formed by relative uplift of several blocks bounded by closely-spaced normal faults (such as faults 2, 3 and 4). This is required if the Kaleköy limestone outcrop is Pliocene. Third, a single normal fault reaches the Earth's surface south of Kaleköy (fault 2), with the whole escarpment in its footwall. This is my preferred interpretation, as there is no evidence of slumping or faulting within the section.

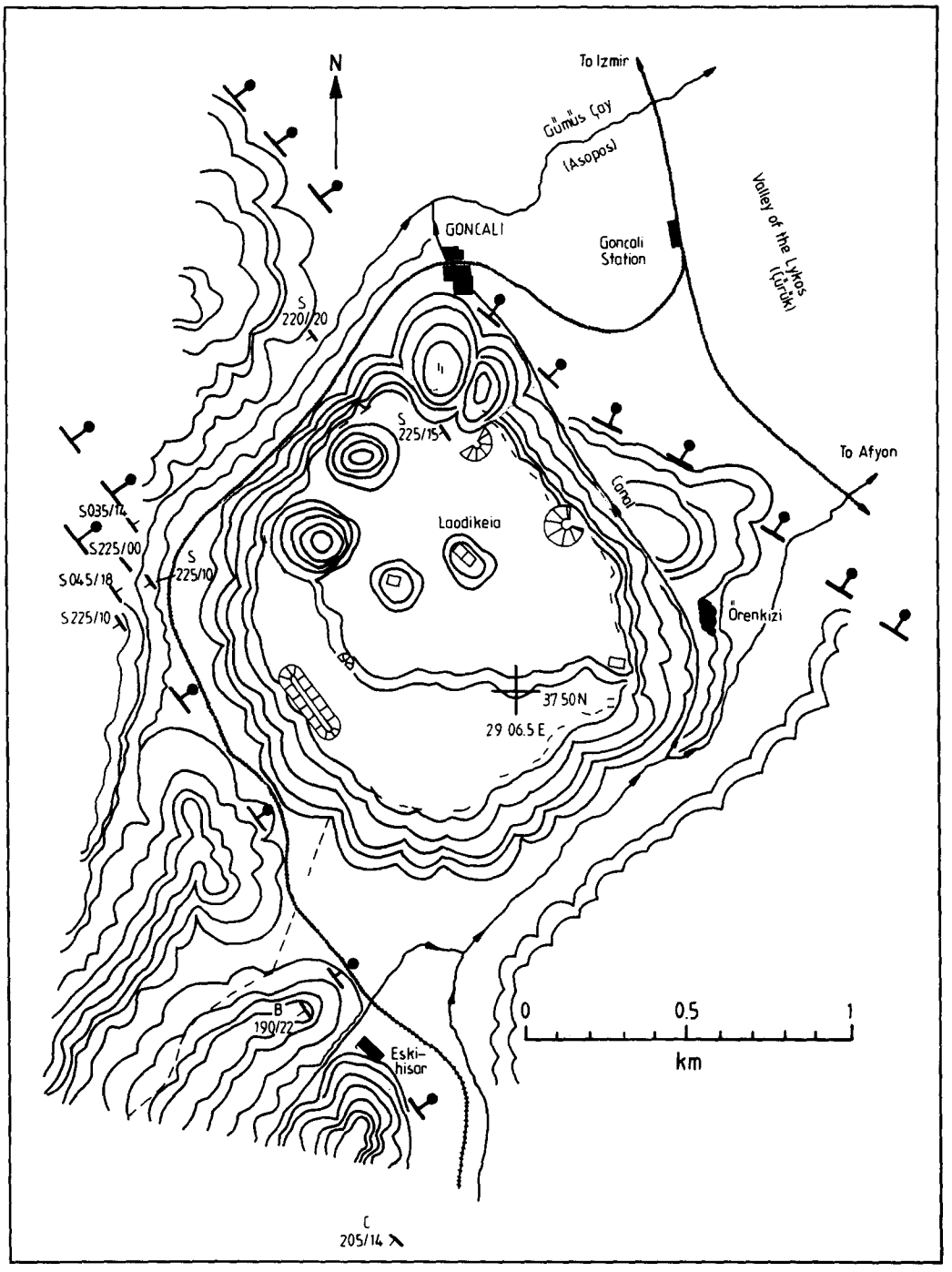

Fig. 5. Detailed map of the vicinity of Laodiceia ad Lycum (Laodikeia), ~5 km north of Denizli. This ancient city was built ~2500 years ago (see e.g. Akurgal 1985, pp. 236–237, Baumgarten 1987, pp. 201–204) on a gently SW-dipping dip slope of Neogene sediment that is uplifted ~60 m above the valley floor that is at ~250 m elevation. Dashed lines indicate interpreted surface traces of normal faults, with hanging-wall ticks. These uplifted sediments are well-exposed at many localities and dip SW at typically 15–20°. Note: (i) the SE-trending dry valley between the Gümüş Çay valley and Eskihisar. Presumably this was once occupied by the stream that now flows northeastward toward Örenkizi; (ii) disturbed pattern of dip in the Gümüş Çay valley, in line with this dry valley. Presumably sediment dip and stream flow have locally been affected by a NW-striking normal fault that follows the dry valley; (iii) the manner in which structures such as the ancient city, a modern irrigation canal, and the railway line that climbs southward to Denizli, follow the fault-related geomorphology. Base map is adapted from fig. 88 of Akurgal (1985). Lines subperpendicular to topographic slope are not contours, but give an impression of topography. Groups of concentric lines bound local topographic highs.

to fault strike, incising the uplifted footwall of the Kaleköy fault (Fig. 2). The greater local elevation of the brackish-water marl in the east indicates faster footwall uplift than elsewhere, which may have exceeded the rate at which all but the largest streams can incise. This is consistent with most extension in the east being on the single Kaleköy fault. Further west, where several normal faults are documented, both within and bounding the uplifted part of the basin (Figs. 2 and 5), footwall uplift rate will not be as large at any locality even though overall extension rate appears greater.

This brackish-water marl unit is thus useful both as a marker to identify uplift and tilting since its deposition, and as an indicator of local conditions. Many results of

this study do not require its absolute age. However, because additional results can be derived if this age is known, I attempt to resolve this, taking account of the different past studies and their discrepancies. Its absence outside the Denizli basin indicates that an isolated depocentre with relatively low elevation already existed when it was deposited, suggesting that some of the present-day topography, which is mostly normal-fault-controlled, already existed. This indicates that this marl is younger than the start of local extension (which is Tortonian or older). It is also older than the overlying Pliocene sediment. Sea level throughout the Mediterranean dropped dramatically (by $\gtrsim$2 km) in Messinian time (7–5 Ma) as a result of a salinity crisis (e.g. Cita 1982). Tectonic activity in the western Mediterranean caused the Strait of Gibraltar to rise above sea level, which stopped the flow from the Atlantic Ocean that maintains water level in the Mediterranean. The transition from marine to brackish conditions at Denizli may well have begun at this time. This suggested Messinian age for the brackish-water marl is consistent with both Gökçen's (1982) study of its microfauna and with the independent Tortonian (or older) dates for the start of extension in western Turkey.

Normal fault morphologies, including indicators of extension sense

Inward-facing escarpments at both margins of the Denizli basin can be readily interpreted as normal-fault footwalls. Several pieces of evidence suggest that the more important faults are along the southwest margin. First, sediments within the basin typically dip SW or SSW. Second, the rugged topography southwest of the basin, in the footwalls of faults at this margin, is more elevated (~1600–2500 m) than at the northeast margin (1200–1700 m), suggesting greater footwall uplift. Much of the region northeast of the basin is instead relatively flat, at ~800–900 m elevation (Fig. 1), and covered with thin Neogene sediment. Third, part of the northeast margin (locality C in Fig. 2), does not appear fault-bounded. Instead, beds locally dip SSW, continuing the sense of tilting observed within the basin.

Normal fault zones can be subdivided into segments that rupture independently in earthquakes (e.g. dePolo *et al.* 1991). Many such segment boundaries occur where normal faults show en échelon steps or abrupt changes in strike. Such fault discontinuities are significant, being likely sites of fault rupture nucleation in large earthquakes. Normal faults in the Denizli region show both types of intersection (Fig. 2). Some similar intersections elsewhere separate normal faults that do not rupture independently (e.g. Westaway 1992a). However, in the absence of knowledge of rupture patterns in large earthquakes (none having occurred near Denizli this century) they can be used as starting points to suggest possible segmentation.

Many ~1–2 km en échelon steps are evident at the detail of mapping, most of which involve ~1–2 km overlaps of adjacent normal faults. Examples are within the uplifted part of the basin south of Sarayköy, between Babadağ and Gerzile at its southern margin, near Pamukkale, and east of Dereköy. The largest is north of Sarayköy, where the northern margin of the Denizli basin steps ~12 km to the left with an ~8 km overlap. The Akküçük Tepe spur of uplifted Neogene sediment between these two fault branches protrudes eastsoutheast into the basin. The longest continuous normal faults shown have length ~30 km, from Tekkeköy to near Denizli and from near Buldan to Pamukkale. These show no evidence for any discontinuity of ~1 km scale. Documentation of any steps and overlaps with dimensions much less than ~1 km will require much more detailed mapping. This apparent ~30 km upper length limit for individual normal fault segments near Denizli exceeds the ~20 km value typical in some other parts of the Aegean (e.g. Roberts & Jackson 1991).

Following Gilbert (1928), normal fault intersections with abrupt changes in strike are called groins if concave and salients if convex towards the hanging wall. In the Denizli region, these are much less numerous than en échelon step type intersections. The largest groin in Fig. 2 is southeast of Çal, where adjacent parts of the Çivril fault at the northwest margin of the Baklan basin differ in strike by ~60°.

One of the most complex normal fault intersections is near Karateke. It involves a ~3 km rightward step between the Gerzile and Honaz faults at the southern margin of the Denizli basin, near which the Honaz fault changes strike by ~30°, turning towards the Gerzile fault. The uplifted spur south of Kaleköy protrudes from this point westnorthwest into the basin interior, bounded by the Okcular fault to the southwest and the Kaleköy fault to the northeast. A continuation of the Kaleköy fault prolongs this spur northwestward past Laodikeia to Üzerlik. It resembles the Traverse Mountain spur between the Salt Lake City and Provo segments of the Wasatch normal fault in the western U.S.A.—one of the most complex segment boundaries documented there (see e.g. fig. 3d of Machette *et al.* 1991)—except most features at Traverse Mountain are roughly a factor of 2 larger. Near Karateke, where the Kaleköy, Gerzile and Honaz faults meet, bed dips are very variable, presumably reflecting complex local deformation at this fault intersection (Fig. 2). Bed dips used to estimate fault tilting are chosen to avoid this and other complex localities.

The major normal fault at the southwestern basin margin is well-exposed at many localities, particularly near its eastern end. No striations are identified on it, but its dip is not observed to differ by more than a few degrees from 45°. The smaller SSW-dipping normal faults at the northern basin margin are less well-exposed, being largely concealed beneath Neogene sediment. The normal faults that approach the Earth's surface within the Denizli basin are also blind for most of their length, and their dips are thus also not directly measurable. To estimate their likely values, Table 1 lists dips of all well-documented normal fault exposures in basement, in parts of western Turkey east of longitude

29°E where extensional strain is small, where normal faults are thus unlikely to have tilted much during extension. Most are ~40–55°, although a few small normal faults are much steeper instead (Tables 1 and 2). Taymaz & Price (1992) recently presented additional fault dip measurements from western Turkey. Their data have not been used in this compilation because they did not distinguish faults in basement and sediment, and did not state which faults are likely to cut the brittle upper crust. They also did not indicate the size of each individual fault exposure, to enable one to judge its significance.

Three fault exposures, where slip sense can be measured, are documented at the southern margin of the Denizli basin, all near its eastern end where limestone basement is exposed (1–3 in Fig. 2; see Table 1 and Appendix 2). The small Okcular (3) and Honaz (2) exposures may be unrepresentative of faulting on a larger scale. Furthermore, given their steep dips, their calculated slip vector azimuths are sensitive to measured rake. The Dereköy exposure (1) is larger; its three sets of values in Table 1 are from points a few hundred metres apart. Slip vector azimuths from this exposure and the focal mechanism of the 13 June 1965 earthquake (Appendix 1) provide the strongest constraints on local extension direction: S24°± 6°W. This is subperpendicular to typical fault strike in the Denizli area, and near the regional average for westernmost Turkey, which Westaway (1990a) determined as S18°± 8°W. Some studies (e.g. Ambraseys & Tchalenko 1972) suggest that normal fault stepping correlates with a component of strike-slip (for example, stepping rightward indicates a component of left-lateral slip). Stepping in the Denizli basin appears random (Fig. 2), leftward in some localities and rightward in others, as is expected with extension subperpendicular to typical fault strike.

Basement is not exposed along any margin of uplifted Neogene sediment in the Denizli basin interior. Published maps (e.g. Pamır 1964) do not interpret these margins as surface traces of normal faults that cut basement at depth. It is critical to later discussion that these localities are accepted as surface traces of major

Table 1. Indicators of extension direction (slip vector azimuth) in the Denizli basin

Description	Strike (°)	Dip (°)	Rake (°)	Azimuth
1. *Reliable data*				
13 June 1965, 20:01 (M_L 5.3) focal mechanism	102	67	−100	S25°W
37°50′N, 29°22′E				
South margin of basin at Dereköy;	280	48	−095	N17°E
37°48′N, 29°23′E; heave ≤1 km; 300 × 50 m	282	49	−104	N33°E
	291	52	−090	N21°E
2. *Less reliable data*				
South margin of basin at Honaz;	310	80	−080	N05°W
37°45′N, 29°16′E; heave ≤1 km; 100 × 40 m				
South margin of basin at Okcular;	120	76	−106	S80°W
37°43′N, 29°13′E; heave ≤1 km; 100 × 5 m				

Documented fault exposures are in limestone with cemented breccia surfaces.

Table 2. Dips of normal faults in localities in western Turkey that have not taken up much extensional strain

Description	Strike (°)	Rake (°)	Azimuth	Dip (°)
1. Typical fault exposures				
South margin of Denizli basin at Dereköy	280	−095	N17°E	48
37°48′N, 29°23′E; heave ≤1 km; 300 × 50 m	282	−104	N33°E	49
	291	−090	N21°E	52
Çatma Dağ fault at Işikli	131	−070	S09°W	54
38°20′N, 29°50′E; heave ~4 km; ~200 × ~30 m	101	−103	S30°W	48
Çatma Dağ fault at Gümüşsu	107	−098	S32°W	58
38°14′N, 30°00′E; heave ~4 km; ~100 × ~2 m				
Kovada fault at Eğridir	350	−116	S60°E	55
37°52′N, 30°52′E; heave ~1 km; ~300 × 100 m				
Kovada fault north of Eğridir	041	−088	S52°E	51
~38°03′N, ~30°49′E; heave ~1 km; size undocumented	034	−078	S76°E	54
	030	−089	S62°E	65
Gelendost fault near Gelendost	215	−076	N73°W	39
38°04′N, 30°59′E; heave ≤1 km; ~100 × 2 m	200	−085	N77°W	40
2. *Unusually steep fault exposures*				
South margin of Denizli basin at Honaz	310	−080	N05°W	80
37°45′N, 29°16′E; heave ≤1 km; 100 × 40 m				
South margin of Denizli basin at Okcular	120	−106	S80°W	76
37°43′N, 29°13′E; heave ≤1 km; 100 × 5 m				

Data for the Kovada fault exposure north of Egridir are from Dumont *et al.* (1979). Other data are from Westaway (1990a) and this study. All fault exposures listed are in limestone, with cemented breccia surfaces.

normal faults, and reasons for this interpretation are therefore briefly stated. First, some of these margins of uplifted sediment have in-line continuations as unequivocal normal faults when they reach the margins of the Denizli basin. The best examples (Fig. 2) are at the western ends of the Dereköy and Okcular fault exposures, and at the western end of the Denizli basin south of the Büyük Menderes River near Çubukdağ. Second, these margins of uplifted sediment in the Denizli basin have very similar form to others elsewhere in western Turkey, which are unequivocally fault-bounded. For example, Fig. 5 can be compared with fig. 5 of Jones & Westaway (1991), which shows the margin of uplifted Neogene sediment in part of the Büyük Menderes fault zone. Landforms in both figures, and their relationship to drainage patterns, are very similar. The Büyük Menderes example is unequivocal: basement is exposed at the margin of uplifted Neogene sediment in the footwall of a normal fault plane that slipped in a historical earthquake.

NEOGENE EVOLUTION

Relationship between faulting and sediment dips

Figure 6 shows three attempts to explain the form of the Denizli basin, along profiles trending N20°E between Gerzile and Pamukkale (Fig. 2). Figure 6(a) assumes that normal-fault bounded blocks rotate as rigid

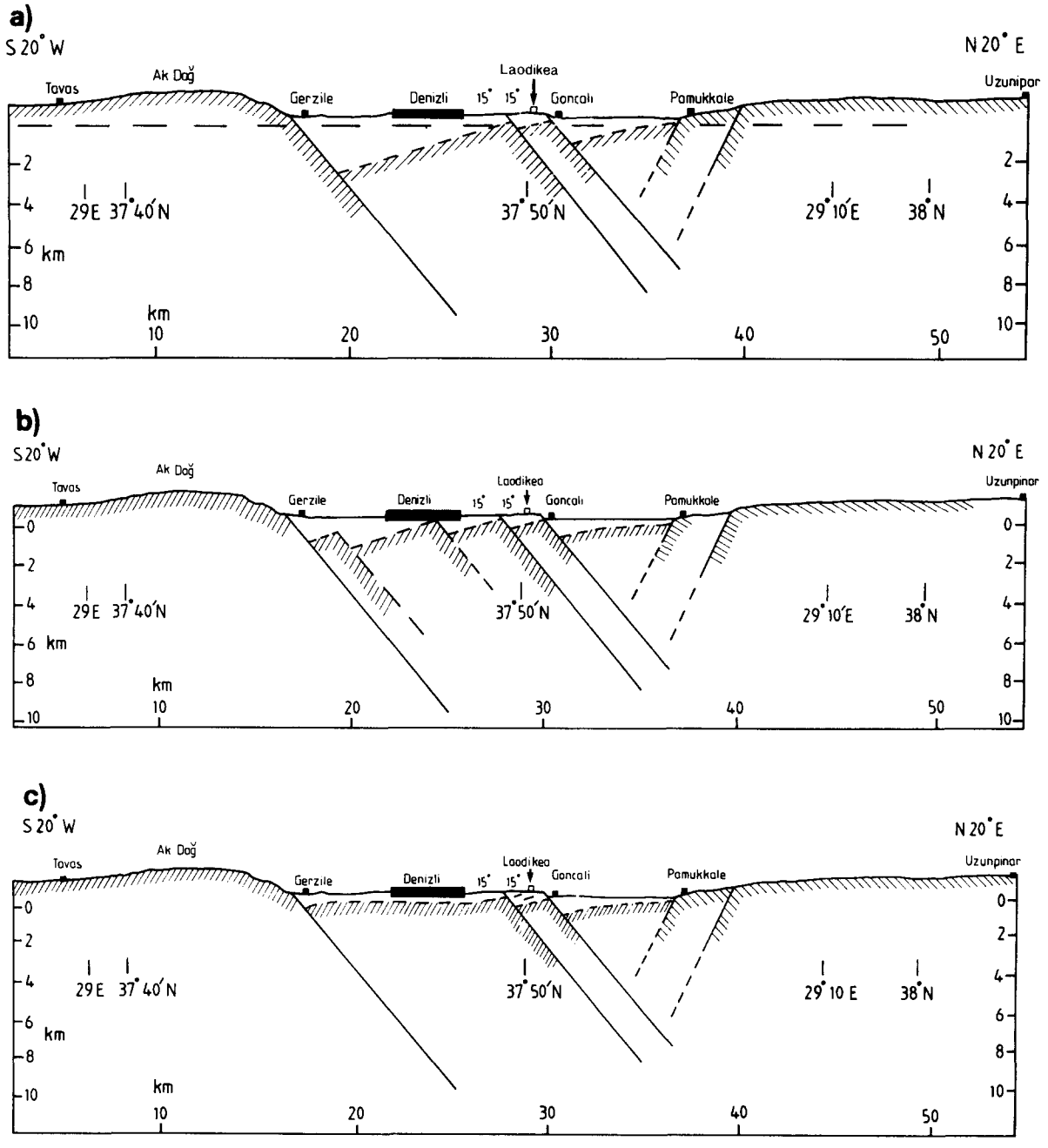

Fig. 6. Schematic cross-section across the Denizli basin showing possible interpretations: (a) tilting by rigid-body rotation; (b) tilting by rigid-body rotation with extra hypothetical faults to reduce basin thickness; (c) (preferred) tilting by distributed vertical simple shear. See text for discussion.

bodies around horizontal axes through the same angle as the bounding faults, following a geometrical method by Westaway (1991). Assuming blocks between the closely-spaced normal faults near the front of the uplifted part of the basin at Goncalı rotate as rigid bodies, with 45° assumed present-day fault dip, the ≳15° SSW tilting observed at the Earth's surface locally requires initial fault dip ≳60°. If the dips of the oldest sediments in this section are regarded as ~20°, as at Kaleköy (Fig. 4), the initial fault dip is 65°, assuming rigid-body rotation. If the 10-km-wide block between Goncalı and Gerzile is also assumed rigid, the uplifted basin near Gerzile needs to be ~3 km thick. This is unlikely, given that further west it is much thinner (its base is exposed at localities J and N in Fig. 2). To avoid this unreasonably thick uplifted basin, Fig. 6(b) is drawn using the same method, but including other NNE-dipping normal faults in the line of section. This does now thin the uplifted basin, but it is unreasonable to introduce these faults when there is no evidence for them in the field.

Figure 6(c) has been drawn assuming distributed vertical simple shear instead. The ~5 km radii of curvature used approximate the value observed in the Kaleköy cross-section (Fig. 4). Such sharp curvature of top basement can readily account for the observed thinness of the uplifted basin. Assuming 45° for the present-day fault dip, the 20° bed tilting requires an initial fault dip of 54° (equation 3). With a present-day fault dip of 50° instead, 20° bed tilting would give an initial fault dip of 57°. With a 45° dip, the NNE-dipping normal fault at Gerzile intersects the SSW-dipping normal fault at Pamukkale at ~5 km depth. For both faults to remain active, instead of one intersecting and locking the other, the base of the brittle layer must be near this level. With a 50° present-day NNE fault dip instead, as observed at Dereköy (Table 1), this reasoning places the base of the brittle layer no deeper than ~7 km. It may be deeper if the SSW-dipping normal faults are steeper, up to a limit of ~8 km. Following this assumption, the steeper the initial fault dip the easier it is to account for the observed substantial sediment tilting and the spacing of NNE- and SSW-dipping normal faults with a realistic thickness of the brittle layer. However, the steeper the normal faults are assumed to be, the less extension is associated with a given amount of throw, and the steeper they are relative to most others in the region (Table 2). Overall, 45–50° seem the likely bounds for the present-day dip of the Kaleköy fault near Goncalı, Laodikeia and Kaleköy, which correspond to 54–57° initial dip for a 20° maximum sediment tilting, assuming vertical shear. This is within the range of typical dips of normal faults farther east in western Turkey (Table 2).

Slumping may potentially cause relatively steep bed dips instead. If one postulates landslides above curved planes near each escarpment, the steep bed dips may be explained without tectonic tilting. Jackson & White (1989) have suggested that soft sediment may detach from basement in this way during extension. I initially regarded this as a possible explanation for the observed dips, being familiar with landslides in Neogene marl and clay elsewhere (e.g. in southern Italy). However, after more detailed study, for the following reasons I now consider this explanation inappropriate for the observed tilting in the Denizli basin. First, no evidence for landsliding, such as scarps at the top, slumps at the foot, or disturbed ground, exist at any locality examined. In particular, there is no evidence for any detachment at localities F and N (Fig. 2) where the base of the uppermost Miocene marl is exposed. Second, bed dips generally decrease upward, moving both from older to younger rocks and up some sections (e.g. at Laodikeia in Fig. 5). Third, the steep bed dip at locality G is in well-consolidated rock and in a locality (the foot of a cliff) where landsliding is unlikely. Fourth, in the Kaleköy section (Fig. 4), similar dips are observed in beds of similar age ~2 km apart. To appeal to landsliding requires either one enormous landslide, which would surely have left evidence of its existence, or two smaller landslides that coincidentally caused tilting through the same angle.

Amount of extension

Following the assumption of distributed vertical simple shear around planar normal faults, the extension across any normal fault equals its heave. The extension across different parts of the Denizli basin can thus be estimated. Throw on the Honaz and Yokuşbası faults in the eastern part of the basin can be roughly estimated as the difference between the footwall elevation (~1400 m) and the ~400 m elevation of the upper Miocene deposits at locality D; it is ~1000 m. Given the ~65–80° dips of these faults, local heave has thus apparently been no more than ~600 m [~1000 m × cos(80°) + ~1000 m × cos(65°)]. Relative to the ~900 m level of the surroundings of the basin, footwall uplift and hanging-wall subsidence are thus roughly equal. Given that this part of the basin has not received much sediment, roughly equal footwall uplift and hanging-wall subsidence relative to the basin's surroundings are expected, as are observed.

The ~1100 m maximum Neogene sediment thickness near Sarayköy and the ~1900 m typical elevation difference between the western part of the mountain range south of the basin and the valley floor suggest ~3000 m of structural relief, of which ~1400 m is on the faults within and north of the uplifted marl (dropping top basement from ~500 m above to ~900 m below sea level) and ~1600 m is on the basement-bounding normal fault near Babadağ. With 45° fault dips this requires 3000 m of heave. The ≳800 m elevation change across the fault at Mahmudiye at the northeast margin of the basin suggests ~800 m of heave, assuming 45° fault dip, making total extension along a section between Babadağ, Sarayköy and Mahmudiye ~3800 m.

Extension across the Gerzile–Pamukkale cross-section can also be estimated. If the basin floor is assumed to slope uniformly upward to the eastsoutheast, from ~900 m below sea level near Sarayköy (consistent with the 1100 m basin thickness and 200 m

elevation of the Earth's surface there) to ~400 m above sea level at Koyunalılar, it would be expected to be ~200 m below sea level in this section, suggesting that locally the basin thickness is ~400 m. This means that total throw (and hence, approximately, heave) on the branches of the Kaleköy fault at Laodikeia is ~700 m. The elevation change across the basin margin from ~1400 to 400 m south of Gerzile indicates ~1000 m of throw (and hence heave, given the 45° fault dip) on this normal fault. Total local heave on NNE-dipping faults is thus ~1400 m. With 800 m of throw and heave on the SSW-dipping faults near Pamukkale, as before, ~2200 m of extension is estimated across this section. Although it is not certain that the basin floor does slope uniformly, this assumption leads to the reasonable result that, relative to the earth's surface in the depocentre, footwall uplift and hanging-wall subsidence for the Kaleköy fault at Laodikeia are roughly equal. Farther east in the vicinity of Koyunalılar, the ~700 m elevation of the upper marl surface near Karateke and the ~400 m elevation of the valley floor imply ~300 m of local throw on the Kaleköy fault. This is consistent with throw on this fault decreasing roughly linearly from ~700 m at Laodikeia to zero at its eastern end.

The ~3 km decrease in heave over ~35 km distance along the Denizli basin is consistent with the rate at which overall extension increases across the major normal faults farther west (Fig. 7). Assuming that this decrease in extension accompanies rigid-body rotation around a vertical axis, it accounts for ~5° ([3/35] × 180°/π) of anticlockwise rotation of the block south of the Denizli basin relative to the block to the north. Extrapolation of this trend eastward predicts that extension in this sense should die out not far east of the eastern end of the Denizli basin. This is consistent with observations that extension sense is different farther east (Westaway 1990a, Taymaz & Price 1992).

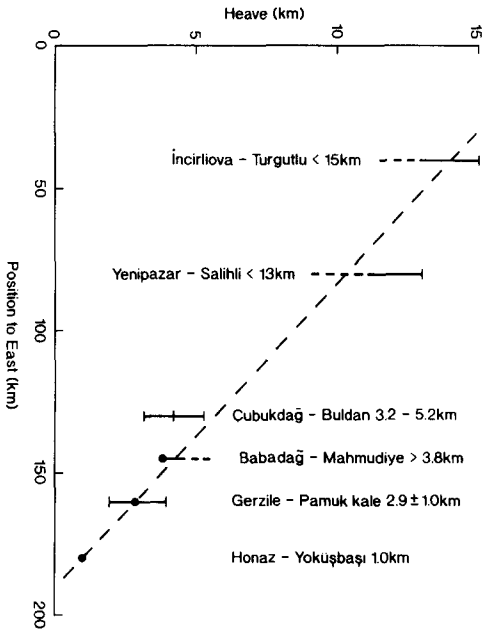

Fig. 7. Graph of eastward decrease in the SSW component of normal fault heave in western Turkey. Eastward distance is measured from the Aegean Sea coast. These observations suggest that southsouthwest heave decreases roughly linearly, reaching zero ~10 km east of the eastern end of the Denizli basin. Heave at localities west of the Denizli basin is the sum across the Büyük Menderes, Küçük Menderes and Alaşehir fault zones, from unpublished work. Assuming vertical shear occurs in the surroundings to normal faults, these variations in heave are equal to variations in extension.

Elevation changes and evolution of normal faulting

The eastern end of the Denizli basin, where extension is minimal, is bounded by a single inward-dipping normal fault at both margins. Both these faults have presumably been active since the start of local extension. However, as already noted, faulting is much more complex farther west, where more extension has occurred. The form of the basin is consistent with extension along its southern flank having migrated northward from the Gerzile and Babadağ faults to the Kaleköy fault and others near it after the brackish-water marl was deposited, causing the later uplift and tilting of this unit. Discussion of this faulting addresses two main issues: the timing of slip on these different faults, and the extent to which local elevation changes relate to their displacements. Some workers have maintained that elevation changes around Aegean normal fault zones relate only to faulting (e.g. Jackson & McKenzie 1983). However, others have suggested that some localities may also require a component of regional uplift (e.g. Roberts & Jackson 1991).

At the end of Tortonian time, after extension began but before the brackish-water marl was deposited, marine conditions existed in parts of the Denizli basin interior (e.g. at locality J), with brackish conditions near its eastern end (e.g. at localities D and G). The link with the sea was presumably via the topographic low along the incipient Büyük Menderes fault zone. The local coastline at the time thus apparently had similar shape to the present-day Gulf of Corinth in central Greece (Fig. 1). The shallow strait at the western end of the Gulf of Corinth formed a drainage threshold, isolating the Gulf from marine lowstands caused by Pleistocene glaciation (Keraudren & Sorel 1987). A threshold west of the Denizli basin would have had a similar effect during the Messinian marine lowstand, maintaining water level within the basin (given the substantial inward drainage via the upstream part of the Büyük Menderes River) when it dropped farther west.

The lack of exposed brackish-water marl west of Çubukdağ suggests that any drainage threshold was nearby. Although Çubukdağ is now at $\gtrsim$100 m elevation, this is not necessarily diagnostic of regional uplift: local sedimentation rate in alluvial fans may simply exceed the hanging-wall subsidence rate. The upper Miocene marine sediments now found in the Denizli basin at ~400 m elevation (e.g. at locality J in Fig. 2), and the younger brackish-water marls at up to ~700 m, have potentially greater significance for regional uplift. However, it seems reasonable to assume initially no regional uplift, and to look for features that are inexplicable following this assumption.

According to Vail *et al.* (1978), at ~2 Ma, immediately before the Pleistocene glaciation, global sea level was ~80 m above its present level, having earlier decreased at 0.003 mm yr^{-1}. If so, immediately before the ~7 Ma start of the Messinian Mediterranean lowstand, when deposition of the Denizli brackish-water marl appears to have begun, sea level—both globally and in the Mediterranean—was ~100 m above its present-day level.

The beach rock at locality J requires 400 m of uplift relative to present-day sea level since Tortonian time, far more than is explicable by the global drop in sea level. This locality is within the footwall of the Kaleköy fault and the other subparallel normal faults along the front of the uplifted part of the Denizli basin near Laodikeia, but is ≳5 km distant. If the elevation of locality J is caused by footwall uplift, the 400 m amount required exceeds the maximum (estimated above) for localities adjacent to these faults. Assuming (as in Figs. 6a & b) that the block behind Laodikeia has tilted uniformly at 15° since the Kaleköy fault became active (consistent with the observed dip at locality J), the uplift required adjacent to this fault is ~400 m + 5 km × tan (15°) or ~1.7 km. This would require massive local footwall erosion, which is not observed. If instead the footwall of this fault has the sharp curvature drawn in Fig. 6(c), negligible uplift would be expected at locality J, regardless of this throw. Either way the present-day elevation of this locality cannot be explained only by footwall uplift. If sea level had remained constant, regional uplift at time-averaged rate ~0.06 mm yr^{-1} for 7 Ma could account for the elevation of locality J. A global sea level drop of 100 m since 7 Ma reduces the required time-averaged uplift rate to ~0.04 mm yr^{-1}. These uplift rates are lower limits, because they will have been partly cancelled by subsidence in the hanging-walls of the Babadağ and Gerzile faults at the southern margin of the Denizli basin during the early stages of extension.

The uppermost marl south of locality J, at ~500 m elevation, was presumably deposited just before extension migrated from normal faults at the southern basin margin to others within the basin. The age of this marl is presumably ~5 Ma (i.e. uppermost Messinian–lowest Pliocene) as it is overlain by thin Pliocene sediments. It thus requires subsequent uplift rate at least ~0.08 mm yr^{-1} (with ~100 m global sea-level drop; ~0.1 mm yr^{-1} with no sea-level drop). If its true age differs from 5 Ma, the required regional uplift rate differs in inverse proportion.

The thin Neogene sediment exposed outside the Denizli basin at ~800–900 m elevation (Fig. 1) is mostly marl and sand; there is no documented Neogene marine sedimentation. Total regional uplift since extension began is thus no greater than ~700–800 m. With uplift rate uniformly ~0.1 mm yr^{-1}, this implies that uplift began at ≲7–8 Ma, after local extension began.

In both the Sarayköy and Gerzile cross-sections slightly more extension is estimated on NNE-dipping faults at the southwestern margin of the basin than on those within the basin. Assuming uniform overall extension rate across the basin, this suggests that extension migrated onto the faults within the basin when it had ≳50% of its present age. This is consistent with extension starting at ~11 Ma and age of the youngest uplifted brackish-water marl 5 Ma. However if, as now seems likely, extension began earlier, then present-day extension rate exceeds the time-averaged rate before faulting migrated northward.

Implications for other extensional basins in western Turkey

This analysis indicates that marl deposited within the Denizli basin has tilted by up to 20° since uppermost Miocene or lowest Pliocene time, when the normal faults within this basin became active. Assuming that these faults now have a dip of 45–50° within the basement, like others nearby, their initial dip was 54–57° for a vertical shear model. The alternative assumption of rigid-body rotation (which can be excluded on other grounds) would predict initial fault dip ~65–70° instead.

Standard theory for the initiation of normal faults in basement, which cut the brittle upper crust, predicts initial dip as a function of their coefficient of friction (Anderson 1951). This theory excludes initial dip above ~70°, as it would require an unreasonably large coefficient of friction. An upper limit of a ~70° dip is indeed observed for normal faults that cut the brittle upper crust and rupture seismically (Jackson 1987). Although near the limit, the initial dips of normal faults that would result from assuming rigid-body rotation at Denizli are not unreasonable. It is interesting to briefly consider other normal faults in western Turkey also.

Other normal fault zones in western Turkey also contain uplifted Neogene basins in the footwalls of the normal faults that are now the most active. As already noted, beds in the uplifted basin along the Büyük Menderes fault zone dip at up to ~26–30°, and the normal faults that cut basement, in whose footwalls this sediment is uplifted, dip at ~45° (e.g. Jones & Westaway 1991, Seyitoğlu & Scott 1992). Lower Pliocene sediment in the Burdur basin typically dips at 13° (Taymaz & Price 1992). Basement is exposed only along part of the fault in whose footwall this sediment has uplifted. Along the principal patch of exposed basement (along-strike length ≲10 km; at Hacılar in the southern part of the basin) this fault has variable dip, but at four of the seven documented localities its dip is in the range 50–62° (Taymaz & Price 1992).

Assuming vertical shear, initial dips of normal faults would have been 56–58° in the Büyük Menderes fault zone and 55–65° at Burdur. Making this assumption, initial normal fault dips in all three basins were apparently similar, ~55–60°, with possibly a slightly higher value at Burdur. In contrast, assuming rigid-body rotation, initial dips would have been 71–75° in the Büyük Menderes fault zone and 63–75° at Burdur. Most of these values are outside the range that is reasonable given Anderson's (1951) theory.

The uplifted basin in the Büyük Menderes fault zone is seldom more than ~4 km wide, and its observed ~2 km thickness (e.g. Jones & Westaway 1991) is explicable in terms of either scheme. In contrast, the uplifted part of the Burdur basin is ~10 km wide, like at Denizli. Assuming rigid-body rotation, maximum thickness of the uplifted Burdur basin would thus be ~10 km × tan(13°) or ≥2 km. From unpublished data, the maximum gravity anomaly across this uplifted basin is barely −15 m gal (S. Price personal communication 1988). Given the ≥500 kg m^{-3} density contrast expected between basement and relatively uncompacted sediment, this anomaly would be expected for a basin with typical thickness barely 1 km. Thus at Burdur rigid-body rotation can be excluded both by calculation of initial fault dip and from the evident thinness of the uplifted basin.

Summary and suggestions for further work

My preferred interpretation of the Neogene evolution of the Denizli region can be summarized as follows (see also Fig. 3). Before extension began, red conglomerate and marl were deposited across the basin area and its surroundings. The region was then subaerial, but presumably had low elevation, because shortly after extension started the interior of the incipient basin dropped below sea level enabling marine limestone to accumulate. Given that the Denizli basin is enclosed to the north, south and east, the connection to the sea in middle–upper Miocene time was presumably via the hanging-wall of the Büyük Menderes fault zone farther west, which was thus also below sea level at the time. The existence of beach deposits, as well as brackish-water limestone of this age in the eastern part of the Denizli basin, indicates that some of it was not fully marine: the palaeocoastline cut across its interior. During Messinian time (~7–5 Ma) sea level in the Mediterranean dropped dramatically, but water level within the Denizli basin was maintained by a threshold at its western end, and the whitish-yellow brackish-water marl was deposited. At the end of Messinian time Mediterranean sea level was restored, but by now the basin interior was above sea level as a result of regional uplift, and subsequent sedimentation has been lacustrine and fluvial. At the same time, or not long afterward, the main active normal faulting moved from the southern margin of the basin to what had been its interior. Uplift began of the brackish-water marl in the southern part of the basin relative to the active depocentre farther north, in the footwalls of these normal faults within the basin. About 4 km of extension has occurred in the western part of the basin, which has present-day width ~24 km. Local extensional strain is thus ~0.2. At least half of this extension has occurred since the active faulting migrated north. If this migration occurred at ~4–5 Ma, subsequent time-averaged local extensional strain rate has been $\sim 8 \times 10^{-16}$ s^{-1}, with time-averaged extensional strain rate over the previous ~10 Ma of extension substantially smaller.

The three main results of this study are as follows. First, taken together the thinness of the sedimentary sequence in the Denizli basin, the substantial dips of Neogene sediments, and the substantial curvature of their profiles, do not support rigid-body rotation. They are consistent with vertical shear instead, as bed tilting exceeds fault tilting.

Second, the typical dip at which major normal faults in the Denizli region formed was no steeper than ~55°, rather than the ~60–70° dip that is sometimes assumed for normal faults in general (e.g. Jackson 1987). However, some small normal faults in western Turkey formed instead with much steeper dip, ~80°, whereas others formed no steeper than 40° (Table 2). Evidently no unique dip exists at which normal faults form, even in this restricted region where the faults considered are all in a single rock type.

Third, the Denizli basin requires ~400–500 m of regional uplift since ~5 Ma, at a time-averaged rate ~0.1 mm yr^{-1}. It thus appears not to satisfy the common assumption that elevation changes associated with Aegean extension are caused only by the isostatic response to displacement on normal faults. Regional uplift may well have also affected other parts of the Aegean region. However, it will be more difficult to identify in most other localities, such as further west in Turkey, where the more rapid extension means that elevation changes caused by faulting are larger and faster. This regional uplift presumably requires influx of material into the lower crust, but its nature and cause remain open to question, and are objectives for future research.

The evident need to further improve understanding of this region by more detailed investigation will probably require the timing of significant tectonic events to be addressed in detail, such as the start of extension and regional uplift, and the migration of faulting. Direct quantification of slip rates on faults, perhaps by trenching, is also desirable.

CONCLUSIONS

Observations of normal faults and dips of Neogene beds in the Denizli basin are assessed for their tectonic significance. The limited extension and low sediment thickness, combined with the relatively steep dips of some uppermost Miocene sediments, up to ~20°, preclude extension having been accommodated by rigid-body rotation of normal-fault-bounded blocks. The evidence is consistent with their tilting having involved distributed vertical simple shear instead. This view, which requires beds to tilt more than adjacent faults, indicates an initial normal fault dip no greater than ~57°. Southsouthwestward extension across this basin decreases from ~4 km near its western end to <1 km near its eastern end, consistent with the regional eastward decrease of extension in this sense across westernmost Turkey. Effects of regional uplift at ~0.1 mm yr^{-1}, which has accompanied this extension, can be dis-

tinguished from elevation changes directly caused by normal feeding.

Acknowledgements—Supported by Natural Environment Research Council grants GR3/6966 and GR3/6967. The following people kindly provided field assistance during January and August–September 1988, April–May, July and August–September 1989, and April–May and September 1990: Kuvvet Atakan, Jan Arger, Günay Çiftçi, Çoskun Sarı, Mujgan Şalk, Ali Pınar, Andrew Heard, Kaan Gürtekin and Malcolm Jones. The British Geological Survey, Edinburgh, provided seismograms of the 13 June 1965 earthquake. I thank Nick Kusznir, Simon Price and Celâl Şengör for helpful discussions, and Gürol Seyitoğlu for a preprint. Ron Bruhn, Ian Stewart and an anonymous reviewer suggested many improvements to the manuscript.

REFERENCES

Aki, K. & Richards, P. G. 1980. *Quantitative Seismology: Theory and Methods*. Freeman, San Francisco.

Akurgal, E. 1985. *Ancient Civilizations and Ruins of Turkey*. Haset, İstanbul, Turkey.

Ambraseys, N. N. 1988. Engineering seismology. *Earthq. Engng Struct. Dyn.* **17**, 1–105.

Ambraseys, N. N. & Tchalenko, J. S. 1972. Seismotectonic aspects of the Gediz, Turkey, earthquake of March 1970. *Geophys. J. R. astr. Soc.* **30**, 229–252.

Anderson, E. M. 1951. *The Dynamics of Faulting* (2nd edn). Oliver & Boyd, Edinburgh.

Ateş, R. 1985. Turkish strong ground motion data acquisition and analysis. *Phys. Earth & Planet. Interiors* **38**, 123–133.

Ateş, R. & Bayülke, N. 1981. Strong motion network of Turkey and analysis of strong motion data. In: *Earthquake Risk Reduction in the Balkan Region, Proc. Regional Seminar on Strong-motion Data Acquisition and Analysis*, Ankara, 9–13 November. Turkish National Committee for Earthquake Engineering, Ankara.

Barka, A. & Kadinsky-Cade, C. 1988. Strike-slip fault geometry in Turkey and its effect on earthquake activity. *Tectonics* **7**, 663–684.

Baumgarten, P. 1987. *Baedeker's Turkish Coast*. Prentice-Hall, Englewood Cliffs, New Jersey.

Becker-Platen, J. D. 1971. Stratigraphic division of the Neogene and oldest Pleistocene in southwest Anatolia. *Newsl. Stratigr.* **1**(3), 19–22.

Cita, M. B. 1982. The Messinian salinity crisis: a review. In: *Alpine–Mediterranean Geodynamics* (edited by Berckhemer, K. H. & Hsü, K.). AGU, Washington, DC, 113–140.

dePolo, C. M., Clark, D. G., Slemmons, D. B. & Ramelli, A. R. 1991. Historical surface faulting in the Basin and Range province, western North America: implications for fault segmentation, *J. Struct. Geol.* **13**, 123–136.

de Tchihatscheff, P. 1867. *Asie Mineure: description physique de cette Contrée, Vol.* 4: *Geologie*. Academy of Sciences, Paris (in French).

Dumont, J.-F., Poisson, A. & Şahinçi, A. 1979. Sur l'existence des coulissements senestres recents a l'extremité orientale de l'arc égéen (sud-ouest de la Turquie). *C. r. Acad. Sci.* **289**, 261–264 (in French with English abstract).

Gilbert, G. K. 1928. Studies of Basin-Range structure. *Prof. Pap. U.S. geol. Surv.* **153**.

Gökçen, N., 1982. The ostracod biostratigraphy of the Denizli-Muğla Neogene sequence, *Bull. Inst. Earth Sci. Hacettepe Univ.* **9**, 111–131 (in Turkish).

Gutniç, M., Monod, O., Poisson, A. & Dumont, J.-F. 1979. Géologie des Taurides occidentales (Turquie). *Mem Soc. géol. Fr.* **137**.

Jackson, J. A. 1987. Active normal faulting and crustal extension. In: *Continental Extensional Tectonics* (edited by Coward, M. P., Dewey, J. F. & Hancock, P. L.). *Spec. Publs geol. Soc. Lond.* **28**, 3–17.

Jackson, J. A. & McKenzie, D. P. 1983. The geometrical evolution of normal fault systems. *J. Struct. Geol.* **5**, 471–482.

Jackson, J. A. & White, N. J. 1989. Normal faulting in the upper continental crust: observations from regions of active extension. *J. Struct. Geol.* **11**, 15–36.

Jones, M., & Westaway, R. 1991. Microseismicity and structure of the Germencik area, western Turkey. *Geophys. J. Int.* **106**, 293–300.

Kaya, O. 1981. Miocene reference section for the coastal parts of west Anatolia. *Newsl. Stratigr.* **10**, 164–191.

Keraudren, B. & Sorel, D. 1987. The terraces of Corinth (Greece): a detailed record of eustatic sea-level variations during the last 500,000 years. *Mar. Geol.* **77**, 99–107.

Koçyiğit, A., 1984. Güneybati Türkiye ve yakin dolanda levha içi yeni tektonik gelisim (in Turkish with English abstract). *Bull. geol. Soc. Turk.* **27**, 1–16.

Kusznir, N. J., Marsden, G. & Egan, S. S. 1991. A flexural cantilever simple shear/pure shear model of continental lithosphere extension: applications to the Jeanne d'Arc basin, Grand Banks, and Viking graben, North Sea. In: *The Geometry of Normal Faults* (edited by Roberts, A., Yielding, G. & Freeman, B.). *Spec. Publs geol. Soc. Lond.* **56**, 41–60.

Le Pichon, X., Lybéris, N. & Alvarez, F. 1984. Subsidence history of the North Aegean trough. In: *The Geological Evolution of the Eastern Mediterranean* (edited by Dixon, J. E. & Robertson, A. W. F.). *Spec. Publs geol. Soc. Lond.* **14**, 727–741.

Machette, M. N., Personius, S. F., Nelson, A. R., Schwartz, D. P. & Lund, W. R. 1991. The Wasatch fault zone, Utah: segmentation and history of Holocene earthquakes. *J. Struct. Geol.* **13**, 137–149.

McKenzie, D. P. 1972. Active tectonics of the Mediterranean region. *Geophys. J. R. astr. Soc.* **30**, 109–185.

Mercier, J. L., Sorel, D. & Vergely, P. 1989. Extensional tectonic regimes in the Aegean basins during the Cenozoic. *Basin Res.* **2**, 49–71.

Pamır, H. N. 1964. *Denizli Sheet of the Geological Map of Turkey*, 1:500,000 scale. Mineral Research and Exploration Institute, Ankara, Turkey.

Pamır, H. N. & Erentöz, C. 1974. *Explanatory Text of the Denizli Sheet of the Geological Map of Turkey*, 1:500,000 scale. Mineral Research and Exploration Institute, Ankara, Turkey.

Poisson, A. 1977. Recherches geologiques dans les Taurides occidentales (Turquie). Unpublished Ph.D. thesis, Université de Paris sud centre d'Orsay.

Price, S. & Scott, B. 1991. Pliocene Burdur basin, SW Turkey: tectonics, seismicity and sedimentation. *J. geol. Soc. Lond.* **148**, 345–354.

Roberts, S. C. 1988. Active normal faulting in central Greece and western Turkey. Unpublished Ph.D. thesis, University of Cambridge.

Roberts, S. C. & Jackson, J. A. 1991. Active normal faulting in central Greece: an overview. In: *The Geometry of Normal Faults* (edited by Roberts, A. M., Yielding, G. & Freeman, B.). *Spec. Publs geol. Soc. Lond.* **56**, 125–142.

Sen, S. & Valet, J. P. 1986. Magnetostratigraphy of late Miocene continental deposits in Samos, Greece. *Earth Planet. Sci. Lett.* **80**, 167–174.

Şengör, A. M. C. 1987. Cross-faults and differential stretching of hanging walls in regions of low-angle normal faulting: examples from western Turkey. In *Continental Extensional Tectonics* (edited by Coward, M. P., Dewey, J. F. & Hancock, P. L.). *Spec. Publs geol. Soc. Lond.* **28**, 575–579.

Şengör, A. M. C., Görür, N. & Saroğlu, F., 1985. Strike-slip faulting and related basin formation in zones of tectonic escape: Turkey as a case study. In: *Strike-slip Faulting and Basin Formation* (edited by Biddle, K. T. & Christie-Blick, N.). *Spec. Publ. Soc. econ. Palaeont. Miner.* **37**, 227–264.

Seyitoğlu, G. & Scott, B. 1991. Late Cenozoic crustal extension and basin formation in west Turkey. *Geol. Mag.* **128**, 155–166.

Seyitoğlu, G. & Scott, B. 1992. The age of the Büyük Menderes graben (west Turkey) and its tectonic implications. *Geol. Mag.* **129**, 239–242.

Sickenberg, O. & Tobien, H. 1971. New Neogene and lower Quaternary vertebrate faunas in Turkey. *Newsl. Stratigr.* **1**,(3), 51–61.

Steininger, F. F. & Rögl, F. 1984. Paleogeography and palinspastic reconstruction of the Neogene of the Mediterranean and Paratethys. In: *The Geological Evolution of the Eastern Mediterranean* (edited by Dixon, J. E. & Robertson, A. H. F.). *Spec. Publs geol. Soc. Lond.* **14**, 659–668.

Taymaz, T., Jackson, J. & McKenzie, D. 1991. Active tectonics of the north and central Aegean Sea. *Geophys. J. Int.* **106**, 433–490.

Taymaz, T. & Price, S. 1992. The 1971 May 12 Burdur earthquake sequence, SW Turkey: a synthesis of seismological and geological observations. *Geophys. J. Int.* **108**, 589–603.

Tezcan, A. K. 1979. Geothermal studies, their present status and contribution to heat flow contouring in Turkey. In: *Terrestrial Heat Flow in Europe* (edited by Cermak, V. & Rybach, L.). Springer, Berlin, 283–292.

Turgut, S. 1988. Observations of the Aegean Sea from the point of view of hydrocarbon exploration. *Bull. Turk. Ass. Petrol. Geol.* **1**, 27–38 (in Turkish with English abstract).

Vail, P. R., Mitchum, R. M. & Thompson, S. 1978. Seismic stratigra-

phy and global changes of sea level. In: *Seismic Stratigraphy* (edited by Payton, C. F.). *Mem. Am. Ass. Petrol. Geol.* **26**, 83–97.
van Eysinga, F. W. B. 1978. *Geological Timetable*. Elsevier, Amsterdam.
Westaway, R. 1987. The Campania, southern Italy, earthquakes of 1962 August 21. *Geophys. J. R. astr. Soc.* **90**, 375–443.
Westaway, R. 1990a. Block rotation in western Turkey: 1. Observational evidence. *J. geophys. Res.* **95**, 19,857–19,884.
Westaway, R. 1990b. The Tripoli, Libya, earthquake of September 4, 1974: implications for the active tectonics of the central Mediterranean. *Tectonics* **9**, 231–248.
Westaway, R. 1991. Continental extension on sets of parallel faults: observational evidence and theoretical models. In: *The Geometry of Normal Faults* (edited by Roberts, A., Yielding, G. & Freeman, B.). *Spec. Publs geol. Soc. Lond.* **56**, 143–169.
Westaway, R. 1992a. Revised hypocentre and fault rupture geometry for the 1980 November 23 Campania–Basilicata earthquake in southern Italy. *Geophys. J. Int.* **109**, 376–390.
Westaway, R. 1992b. Analysis of tilting near normal faults using calculus of variations: implications for upper crustal stress and rheology. *J. Struct. Geol.* **14**, 857–871.
Westaway, R., Gawthorpe, R. & Tozzi, M. 1989. Seismological and field observations of the 1984 Lazio–Abruzzo earthquakes: implications for the active tectonics of Italy. *Geophys. J.* **98**, 489–514.
Westaway, R. & Jackson, J. A. 1987. The earthquake of 1980 November 23 in Campania–Basilicata (southern Italy). *Geophys. J. R. astr. Soc.* **90**, 375–443.
Westaway, R. & Kusznir, N. J. 1990. Neogene evolution of the Aegean region. (Abs.) *Trans. Am. Geophys. Un.* **71**, 1634.
Westaway, R. & Kusznir, N. J. In press. Fault and bed 'rotation' during continental extension: block rotation or vertical shear? *J. Struct. Geol.*
Westaway, R. & Smith, R. B. 1989a. Strong ground motion in normal faulting earthquakes. *Geophys. J.* **96**, 529–559.
Westaway, R. & Smith, R. B. 1989b. Source parameters of the Cache Valley (Logan), Utah, earthquake of 30 August 1962. *Bull. seism. Soc. Am.* **79**, 1410–1425.

APPENDIX 1
THE DENIZLI EARTHQUAKE OF 13 JUNE 1965

The Denizli basin has experienced two moderate-sized earthquakes in the past 30 years: at 20:01 on 13 June 1965 and at 01:12 on 19 August 1976. The 1976 event (M_L ~5.0) occurred directly beneath Denizli city, and is of interest partly because it generated the first record of ground acceleration for any western Turkish earthquake (Ateş & Bayülke 1981, Ateş 1985, Westaway & Smith 1989a). Its location is constrained mainly by the distribution of damage, which was concentrated east of Denizli city centre (Ateş & Bayülke 1981). An epicentre in this position is consistent with a 5–10 km deep hypocentre on a patch of the Gerzile normal fault at the southern margin of the Denizli basin, assuming this fault dips at ≳45°. This 1976 event is below the usual threshold for straightforward determination of a first-motion focal mechanism taken from teleseismic records. I have indeed been unable to obtain enough legible records for it, and consequently can provide no seismological confirmation that it did involve normal faulting. However, in view of its tectonic setting this does seem a reasonable assumption (see also Westaway & Smith 1989a). This study concentrates instead on the 1965 Honaz event that being larger (M_L 5.3) is more important in terms of tectonic deformation and also easier to study. Normal-faulting earthquakes of similar size elsewhere take up deformation in the same sense at less frequent, larger, events in the same regions (e.g. Westaway 1987, 1990b, Westaway *et al.* 1989, Westaway & Smith, 1989b). I first locate this 1965 event relative to the 1976 earthquake, showing that it most likely occurred ~4 km west of Kaklık near the eastern end of the Denizli basin (Fig. 2). Second, I constrain its source orientation using both P- and SH-wave polarities, providing a revised focal mechanism that supercedes an earlier result by McKenzie (1972). Third, I discuss the joint interpretation of these results, which indicate that this 1965 event occurred on a patch of a steep S-dipping normal fault at the northern margin of the basin (Fig. 2).

Location

Table A1 lists locations by seismological agencies and others for the 1965 and 1976 events. Previous studies (e.g. Westaway & Jackson 1987) establish that agency locations for eastern Mediterranean earthquakes are likely to be in error, potentially by tens of kilometres in hypocentral co-ordinates, and by 1 s or more in origin time. On their own, they are thus a weak basis for associating earthquakes with particular active faults. The macroseismic epicentre of the 1965 event by Ambraseys (1988) is at Honaz (Fig. 2), after which it was named, at the southern margin of the eastern Denizli basin. However, damage in 1965 was concentrated further north, within the eastern part of the basin and on the S-facing slopes on its north side (Ambraseys 1988), suggesting that this earthquake more likely occurred further north.

The macroseismic epicentre that I have determined using the contour map of earthquake damage in 1976 (from Ateş & Bayülke 1981) is listed in Table A1 also. This map showed a roughly circular area with a radius of ~1.2 km where seismic intensity exceeded 6, centred at the listed position that is just east of Denizli city centre. Within this, a smaller area where intensity exceeded 7 was also identified. This macroseismic location appears more reliable than the instrumental locations that are ~10 km further southwest, and are thus outside the Denizli basin and consistent with no documented normal fault. I use it as a starting point for locating the 1965 event.

The 1965 event is located relative to this macroseismic location for the 1976 event using the relative timing of P-waves recorded for both events by seismograph stations within ~1000 km. If one assumes either that both events occurred at the same focal depth, or differences in focal depth are small compared with their horizontal separation, one may locate earthquakes relative to one another using theory developed by Westaway (1987). Relative arrival time for any station will in general depend on the take-off angle and azimuth of P-waves travelling to that station, as well as on the relative azimuth of the two events. If one uses only relatively close stations (such as those within ~800 km that record Pn-wave arrivals that are Moho refractions, and others not much further away where P-waves dive gently into the uppermost mantle), take-off angle is constant to a good approximation and relative arrival time for any station depends only on the difference in azimuth between the raypath and a line between the two epicentres. Relative arrival time is thus expected to vary sinusoidally with raypath azimuth, the phase of the variation giving the relative azimuth of the epicentres.

Relative arrival time is also affected by two types of error. First, arrivals may be picked incorrectly on seismograms, and, second, timing of seismographs may be in error. Without access to seismograms, nothing can be done directly about these sources of error, although picking errors are likely to be smallest at relatively close stations where events are recorded most strongly. Furthermore, inspection of the relevant equations in Westaway (1987) indicates that for a given horizontal separation of two events, relative arrival time is typically largest for close stations, at which 'real' arrival time differences caused by differences in epicentral position are most likely to predominate over spurious differences caused by timing and picking errors. Restricting oneself to data from only the closest stations thus offers potential advantages for relative earthquake location compared with the older method by Westaway (1987), even though it may reduce the number of P-wave arrival time data used. For more detailed analysis of the errors associated with this new method see Westaway (1992a).

Figure A1 shows relative arrival time vs azimuth for the 10 seismograph stations within 1000 km that recorded both events. This unusually small number of common stations arose through the lack of

Table A1. Locations of the 1976 and 1965 Denizli events

Origin time (s)	Latitude (° ± km)	Longitude (° ± km)	Depth (km)	Ref.*
13 *June* 1965, 20:01				
48.0	37.8	29.3	16	NEIS
50.8 ± 0.1	37.85 ± 2.6	29.32 ± 1.7	33 ± 3.2	ISC
	37.75	29.3		A88
47.0	37.84 ± 4.0	29.37 ± 4.0	10	This study
19 *August* 1976, 01:12				
36.7	37.7	28.97	10	NEIS
40.0 ± 1.0	37.71 ± 3.3	29.00 ± 2.4	20 ± 8.0	ISC
	37.78 ± 1.0	29.09 ± 1.0		AB81
38.0	37.78 ± 1.0	29.09 ± 1.0	10	This study

*Abbreviations: ISC, International Seismological Centre; NEIS, U.S. National Earthquake Information Service and its predecessors; A88, Ambraseys (1988); AB81, Ateş & Bayülke (1981).

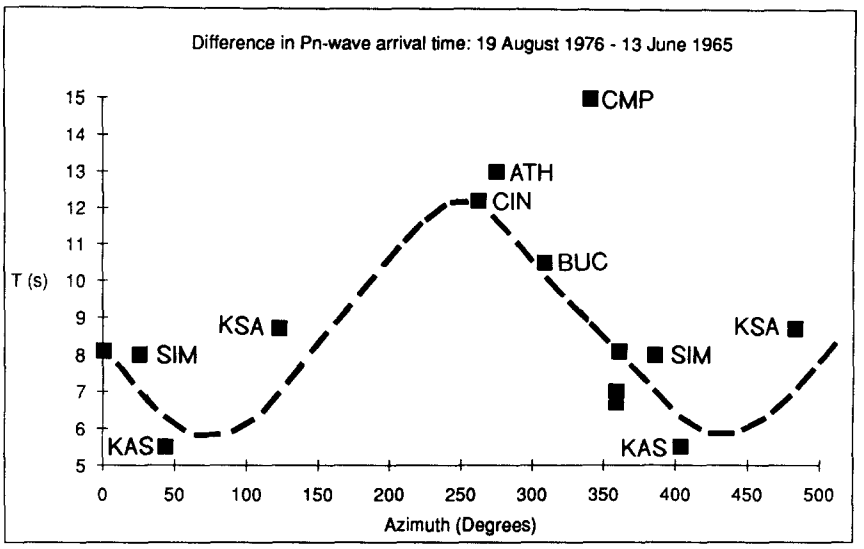

Fig. A1. Plot of difference in the second part of P-wave arrival time for the 1965 and 1976 earthquakes vs azimuth for the 10 stations within ~1000 km that reported both events: CIN (Δ = 0.73°, α = 262°, δt = 67.0–54.8 s), IST (Δ = 3.33°, α = 359°, δt = 39.2–32.5 s), ISK (Δ = 3.35°, α = 001°, δt = 38.1–30.0 s), ATH (Δ = 4.19°, α = 275°, δt = 57.0–44.0 s), KAS (Δ = 5.19°, α = 044°, δt = 65.0–59.5 s), KSA (Δ = 6.81°, α = 123°, δt = 26.7–18.0 s), BUC (Δ = 7.05°, α = 309°, δt = 35.0–24.5 s), CMP (Δ = 8.11°, α = 340°, δt = 52.0–37.0 s), SIM (Δ = 8.19°, α = 026°, δt = 46.0–38.0 s) and KIS (Δ = 9.30°, α = 359°, δt = 61.0–54.0 s). Here Δ and α are the distance and azimuth of the station from the ISC epicentre for the 1976 event, and δt is the difference in the second part of P-wave arrive time for the 1965 event minus the 1976 event. The sine curve fitted by eye is consistent with the two epicentres being 24 km apart with the 1965 event at azimuth 165° relative to the 1976 event, and indicates that the second part of origin time was ~9 s later in 1965 than in 1976, supporting the estimated origin times in Table A1.

continuity of operation of many stations in Turkey and Greece: between 1965 and 1976 a large proportion of stations were discontinued and replaced by others elsewhere. One station (CMP) is inconsistent with the rest, presumably because of a picking or timing error. A sine curve fitted by eye through the remaining data has peak to peak amplitude 6 s (suggesting epicentral separation 24 km given Pn velocity 8 km s^{-1}) and a phase that suggests the 1965 event was at azimuth 165° relative to the 1976 event. This implies that the 1965 event occurred at latitude 37.84°, longitude 29.37°, near the eastern end of the Denizli basin. Uncertainty in phase of this sine curve can be estimated as ~10°, which, given the 24 km separation, suggests ± ~4 km uncertainty in epicentral position in the azimuthal direction. The ~1 s uncertainty in peak to peak amplitude suggests ± ~4 km uncertainty in the radial direction also.

Focal mechanism

Figure A2(a) shows the focal mechanism for the 1965 event determined from McKenzie (1972) using P-wave polarities. Its nodal planes have strike 101° dip 70° and rake −090°, and strike 281°, dip 20° and rake −090°. Most of the stations used by McKenzie (1972, fig. 21a) have been identified, and a revised focal mechanism using these and other P- and SH-wave data are shown in Figs. A2(b)&(c). SH-wave polarities were picked only at stations where raypath azimuth was subperpendicular to one of the horizontal components of ground motion. Polarities are expressed using the convention of Aki & Richards (1980, p. 115), where positive SH-wave polarity involves motion to the right when looking along the raypath away from the

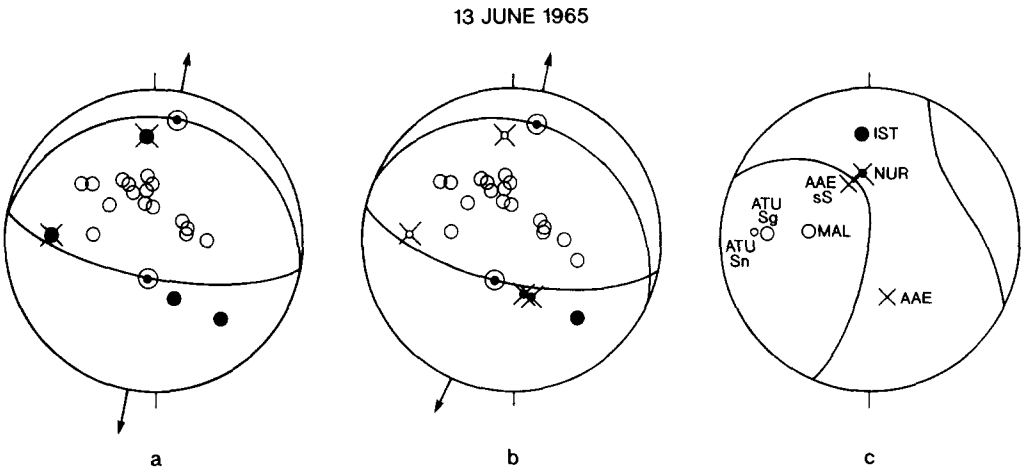

Fig. A2. Focal mechanisms for the 1965 event. (a) From McKenzie (1972) using P-wave polarities including: compressions at AAE and JER; dilatations at ANP, BAG, CMC, COL, COP, KEV, KON, KTG, MAL, NDI, NOR, NUR, SHK, STU, TRI and VAL; and a nodal compression at ATU. (b) Determined here using P-wave polarities (a compression at JER; dilatations at ANP, BAG, CMC, COL, COP, KEV, KON, KTG, MAL, NDI, NOR, NUR, SHK, STU, TRI and VAL; nodal weak compressions at AAE and NAI; and nodal weak dilatations at ATU and IST) and consistent with (c). (c) Determined here using SH-wave polarities (positive at IST; negative at MAL; and nodal weak positive at NUR. Nodal S- and sS-pulses were observed at AAE; and at ATU an initial weak negative pulse—interpreted at Sn—is followed by a stronger negative pulse—interpreted as Sg) and consistent with (b).

source towards the station. Two of my P-wave polarity picks (at ATU and IST) disagree with those by McKenzie (1972). These are at nodal stations where he reported polarity violations. At AAE, I interpret the compressional polarity reported by McKenzie (1972) as nodal, although this difference does not affect the solution.

My revised focal mechanism has a S-dipping nodal plane with strike 102°, dip 67° and rake −100°, making slip vector azimuth S25°W if this plane was the fault plane. This mechanism is tightly constrained when P- and SH-wave polarities are used together. Rake, and hence slip vector azimuth, is most tightly constrained by the nodal positive SH-wave polarity at NUR, which is unequivocal. Features of earthquake sources such as multiple fault ruptures or slip on a fault with variable orientation can be revealed by teleseismic body-wave modelling. However, the moderate size of this event makes it unlikely to have involved these complexities. The relatively small amplitudes of its teleseismic body-waveforms would also be difficult to digitize accurately and in digitized form would have low signal to noise ratios. Modelling them would consequently be unlikely even to give a source orientation that is as well-constrained as it possible using polarities alone, let along provide any improvement.

Interpretation

The 1965 epicentre is near the eastern end of the Denizli basin, west of Yoküşbaşı (Fig. 2), roughly halfway between the escarpment at the northern edge of the basin, which I suggest is a S-dipping normal fault, and the western end of the N-dipping Dereköy normal fault. It seems likely that this event nucleated at a depth of ~5 km or more, possibly at the point where these N- and S-dipping normal faults intersect at depth. The S-dipping nodal plane of the focal mechanism has similar strike to the S-facing escarpment, and is most likely the fault plane. With this choice of nodal plane, slip vector azimuth resembles very closely that measured at Dereköy. If so, the faults bounding both margins of the Denizli basin take up extension towards the same azimuth, which is reasonable.

APPENDIX 2
DOCUMENTATION OF FIELD LOCALITIES

This Appendix describes localities that are mentioned in the text and shown in Fig. 2, where significant field observations are made. Information for access is also provided.

Fault exposures 2 and 3 are obvious from Honaz and Dereköy, which are signposted from the Denizli–Burdur road (320). The Denizli–Antalya road (350) passes 1 km from the Okcular fault exposure (1), but on the wrong side of the Okcular ravine. This exposure is accessible by leaving the Denizli–Honaz road 3 km southwest of Koyunalılar on a dirt road that passes east of Emirazizli and through Karateke, turning left at a crossroads ~2 km west of Karateke and continuing south for 3 km. The dirt road that continues ahead west of Karateke leads to Denizli via locality I. It joins road 350 opposite the Karayolları depot, ~1 km south of its junction with road 320 in Denizli city centre.

Between A and B, ~2–5 km north of Yoküşbası on the Denizli–Çivril road (595), between kilometre markers 595-13-045 (at A) and 595-13-042 (at B), the Aquitanian red conglomerate and marl are exposed. This exposure covers much of the elevated area between the Denizli and Baklan basins. Dip is variable, as may be expected near the intersection of several later normal faults with different orientations: subhorizontal in some localities but up to 35° towards 255° near the northern end of the exposure. A is ~5 km north of the junction of roads 595 and 320 at Kaklık.

C is an exposure in a stream channel at the northern margin of the Denizli basin north of Koyunalılar. Unconsolidated conglomerate, marl and sand dip at 5° towards 210°, and unconformably overlie well-consolidated conglomerate that dips at 10° towards 030°. This site is accessible on a dirt road that leaves road 320 just east of kilometre marker 320-04-010, where this road crosses the Dogüş River (a tributary of the Aksu), ~500 m west of Denizli industrial estate. This dirt road heads northeast until it crosses the Acı River, before turning west for ~500 m.

D is an exposure of well-consolidated limestone with bulrush fossils (most likely middle–upper Miocene) that dips at 5° towards 040°. It is at ~400 m elevation on road 320 near kilometre marker 320-04-018, ~10 km west of the Kaklık junction. E–F comprise a series of exposures, mostly of limestone, at the southern edge of the Denizli basin near Emirazizli and Karateke, on the route to fault exposure 1. East of Emirazizli a ~100 × ~100 m outcrop of medium hard sandy limestone (middle–upper Miocene?) has a dip of 13° towards 180°. Similar limestone in Karateke village has a dip of 18° towards 010°. At F, ~500 m south of the left turn to locality 1, the unconformity between the uppermost Miocene marl and the medium hard (middle–upper Miocene?) limestone is well exposed. This unconformity dips WNW at a shallow angle and shows no evidence of slumping or other disturbance. About 100 m further east the older unconformity between this medium hard limestone and the much harder Mesozoic crystalline limestone is also exposed.

At G, at Koyunalılar, the Aksu River emerges from a ~100 m deep gorge in the floor of the eastern part of the basin, entering the lower-lying western part that is below ~250 m elevation. Near the junction for Honaz on road 320, near kilometre marker 320-04-009, medium hard limestone with bulrush fossils, like at D, is exposed, with a dip of 28° towards 228°. Exposure is clearest south of the Honaz road just before it crosses the Denizli–Afyon railway and climbs out of the gorge.

H–I is the cross-section from Kaleköy to Karakurt in Fig. 4. South of Kaleköy a dirt road climbs the footwall of the Kaleköy fault in Neogene sediment from ~300 to ~550 m elevation. Near the base of this escarpment, limestone with bulrush fossils is exposed, with a dip of 18° towards 218° (locality H). Marl is exposed higher, but with no clear dip indicators. At the top of the escarpment, conglomerate units that are several metres thick dip at 20–24° towards 220°. Farther south-southwest, the road descends gently for ~1 km on a dip-slope, before joining the dirt road from Karateke to Denizli. One kilometre west of its junction with the road from Kaleköy, marl is interbedded with conglomerate sheets. The marl weathers vertically, whereas the conglomerate weathers at a slope, enabling discontinuities to be readily traced and their dip measured: 5° towards 040° (locality I).

At J, at ~400 m elevation, south of road 320, ~5 km west of Denizli city centre and ~10 km east of Beylerbeyi, a sign saying "Borusan borude kalite damgası" marks a raised beach: cemented sand and pebbles, with mollusc fossils and shell fragments, which dips at 15° towards 190°. This unit underlies the brackish-water marl to the south and is thus presumably of middle–upper Miocene age.

L marks the ancient city of Laodicaea ad Lycum (Laodikeia) (Fig. 5). For access, leave road 320 at the junction for Pamukkale and turn left ~1 km further north. The headwaters of the stream that reaches the depocentre at Örenkizi appear to have flowed into the Gümüş Çay until the recent past, when captured by a stream that incised the uplifting spur southward from Örenkizi. This river capture resembles another reported by Jones & Westaway (1991) in an equivalent locality further west in Turkey. Similar processes are probably common in localities where unconsolidated sediments are uplifting.

M marks the northern end of uplifted Neogene sediment along the Sarayköy-Babadağ road, ~2 km south of the Denizli–İzmir railway at Sarayköy. Unconsolidated sand locally dips at 26° towards 016°. Marl further south dips SSW at typically ~8°, with occasional localities with steeper (~30°) NNE dip. These relatively steep NNE dips are interpreted as points where sediment drapes across NNE-dipping normal faults. At N, this road crosses a gorge that has incised to the base of the marl at ~450 m elevation. Hard limestone below this unconformity dips NE at ~50°. The lowest metre of marl contains numerous rounded clasts of Menderes schist that fine upward.

The Büyük Menderes River drops from 750 to 150 m elevation between the Baklan basin at Asağiseyit and the Denizli basin at Mahmudiye (Fig. 2). Marl is exposed within the Baklan basin, whose flat surface is at 800 m elevation. The 50 m deep Büyük Menderes gorge in the western Baklan basin has incised to limestone basement, indicating that this basin is very shallow near its northwestern edge. Near the Çal groin this gorge incises the footwall of the Çivril fault that bounds the northwestern margin of the Baklan basin. The footwall escarpment of this fault is typically ~200 m high, rising to ~1000 m elevation. The Çivril fault has its footwall ~100 m above, and its hanging-wall ~100 m below, the ~900 m typical level of its surroundings.